NASA Contractor Report 145301

Evaluation of a Large Capacity Heat Pump Concept for Active Cooling of Hypersonic Aircraft Structure

L.L. Pagel and R.L. Herring

McDonnell Douglas Corporation
McDonnell Aircraft Company
St. Louis, Missouri

Prepared for
Langley Research Center
under Contract NAS1-14981

National Aeronautics
and Space Administration
Scientific and Technical
Information Office

1978

Page
Intentionally
Left Blank

1. Report No.	2. Government Accession No.	3. Recipient's Catalog No.
NASA CR- 145301		

4. Title and Subtitle	5. Report Date
EVALUATION OF A LARGE CAPACITY HEAT PUMP CONCEPT FOR ACTIVE COOLING OF HYPERSONIC AIRCRAFT STRUCTURE	February 1978
	6. Performing Organization Code
7. Author(s)	8. Performing Organization Report No.
L. L. Pagel and R. L. Herring	
	10. Work Unit No.
9. Performing Organization Name and Address	
McDonnell Douglas Corporation P.O. Box 516 St. Louis, Missouri 63166	11. Contract or Grant No. NAS1-14981
	13. Type of Report and Period Covered Contractor Report
12. Sponsoring Agency Name and Address	14. Sponsoring Agency Code
National Aeronautics & Space Administration Washington, D.C. 20546	

15. Supplementary Notes

Langley technical monitor: Pierce L. Lawing

16. Abstract

This report presents results of engineering analyses assessing the conceptual feasibility of a large capacity heat pump for enhancing active cooling of hypersonic aircraft structure. At present, considerable thermal shielding of the aircraft's aluminum structure is required. That is, due to the low operating temperature of aluminum, only a fraction of the heat sink capacity available in the hydrogen fuel can be utilized, necessitating thermal shielding and a corresponding reduction in airframe cooling requirements. The present study identifies a unique heat pump arrangement which permits cooling the structure of a Mach 6 transport to aluminum temperatures without the aid of thermal shielding. The selected concept is compatible with the use of conventional refrigerants, with Freon R-11 selected as the preferred refrigerant for the conditions of this study. Condenser temperatures were limited to levels compatible with the use of conventional refrigerants by incorporating a unique multipass condenser design, which extracts mechanical energy from the hydrogen fuel, prior to each subsequent pass through the condenser. Program results show that it is technically feasible to use a large capacity heat pump in lieu of external shielding. Additional analyses are required to optimally apply this concept. Study results and conclusions are discussed in the body of the report; analysis methods used are presented in the Appendix.

17. Key Words (Suggested by Author(s))	18. Distribution Statement
Aluminum Actively Cooled Panel Heat Shields Hypersonic Aircraft Heat Pump Power Turbines Hydrogen Fuel	Unclassified - Unlimited

19. Security Classif (of this report)	20. Security Classif (of this page)	21. No. of Pages	22. Price
Unclassified	Unclassified	49	

FOREWORD

This report was prepared by McDonnell Aircraft Company (MCAIR), St. Louis, Missouri, for the Langley Research Center of the National Aeronautics and Space Administration. The objective of this program was to add to the existing technology base for active cooling of hypersonic aircraft structure by assessing a large capacity heat pump concept, a unique method of increasing the amount of hydrogen heat sink available for structural cooling. The program was conducted in accordance with NASA RFP 1-05-[illegible] 3734.0128 and McDonnell's Technical Proposal, MDC A4755. Customary units were used in performing the engineering analyses discussed herein. Study results were converted to the International System of Units (SI) for the final report.

Mr. Ralph L. Herring was the MCAIR Program Manager, with Mr. LaVerne L. Pagel as Principal Investigator.

TABLE OF CONTENTS

Section	Page
FOREWORD	iv
TABLE OF CONTENTS	v
LIST OF ILLUSTRATIONS AND TABLES	vi
SUMMARY	1
INTRODUCTION	5
LIST OF SYMBOLS	7
BASELINE AIRCRAFT CHARACTERISTICS	9
POWER EXTRACTION	13
HEAT PUMP ANALYSES	17
EFFECT OF IMPROVED AERODYNAMIC EFFICIENCY	27
IMPACT ON AIRCRAFT PERFORMANCE AT L/D = 4.66 AND 5.83	31
CONCLUSIONS	35
RECOMMENDATIONS	37
APPENDIX - METHODOLOGY	39
REFERENCES	49

LIST OF ILLUSTRATIONS

Figure	Title	Page
1	Baseline Aircraft	2
2	Heat Pump Enhances Active Cooling of Aircraft Structure	3
3	Schematic of Fuel/Coolant System for Mach 6 Baseline Aircraft (L/D = 4.66)	11
4	Power Turbine Output vs Hydrogen Fuel Pressure for Mach 6 Baseline Aircraft	14
5	Power Characteristics - Heat Pump with Multipass Condenser Cools Mach 6 Bare Aluminum Aircraft	22
6	Selected Heat Pump/Fuel System Arrangement for Mach 6 Bare Aluminum Aircraft (L/D = 4.66)	23
7	Schematic of Fuel/Coolant System for Mach 6 Bare Aluminum Aircraft with 25% Improvement in Cruise L/D	28
8	Heat Pump Performance	43

LIST OF TABLES

Table	Title	Page
1	Baseline Aircraft Characteristics	10
2	Characteristics of a 22.4 MW (30,000 HP) Hydrogen Power Turbine	15
3	Concept 1 Heat Pump/Fuel System Characteristics	18
4	Heat Pump with Multipass Condenser and Power Extraction Cools Mach 6 Bare Aluminum Aircraft	
	a. SI Units	20
	b. Customary Units	21
5	Component Mass and Volume Breakdown for Selected Heat Pump System	25
6	Heat Pump vs Shielding Increases Aircraft Mass	26
7	Aircraft Performance	32
8	Cruise Fuel Flow Sensitivity	33
9	Freon R-11 Refrigeration Cycle	45
10	Equations Defining the Mass of Active Cooling System Elements	47

SUMMARY

A detailed study was conducted to conceptually design and evaluate the use of a large capacity heat pump as a means of increasing the amount of hydrogen heat sink available for active cooling of hypersonic aircraft structure. Specific objectives of this program were:

(a) Evaluate feasibility of using a heat pump concept to enhance active cooling,

(b) Assess the advantages or disadvantages of using this system, relative to current active cooling concepts for aluminum aircraft (thermal shielding), and

(c) Determine whether, by using the heat pump to increase the available fuel heat sink, a bare (unshielded) aluminum hypersonic transport can be actively cooled.

The baseline aircraft configuration used throughout the study was a Mach 6 actively cooled, liquid hydrogen fueled transport (reference 1) with a cooled structural area of 2980 m^2 (32,134 ft^2) and 5.9 Mg (12,900 lbm) of external shielding. The aircraft (figure 1) carries 200 passengers with a mission range of 9200 km (4968 NM). Airframe and engine cooling requirements used throughout the study were obtained from references 1 and 2 respectively.

The design philosophy for use of a heat pump to enhance active cooling of the aircraft structure is illustrated in figure 2. As shown, the airframe structure is cooled with a 60/40 mass solution of ethylene glycol and water. The airframe heat load $\dot{Q}_s$ is transported by the closed loop coolant system and rejected to the hydrogen fuel via the hydrogen/glycol heat exchanger ($\dot{Q}_{H/X}$) and the heat pump ($\dot{Q}_e$). Without a heat pump, external shielding would be required to limit the airframe heat load to a level consistent with the hydrogen heat sink available through direct heat transfer in the heat exchanger. The heat pump rejects heat to the hydrogen at temperatures in excess of heat exchanger outlet temperature T_4, thereby increasing the available heat sink for structural cooling.

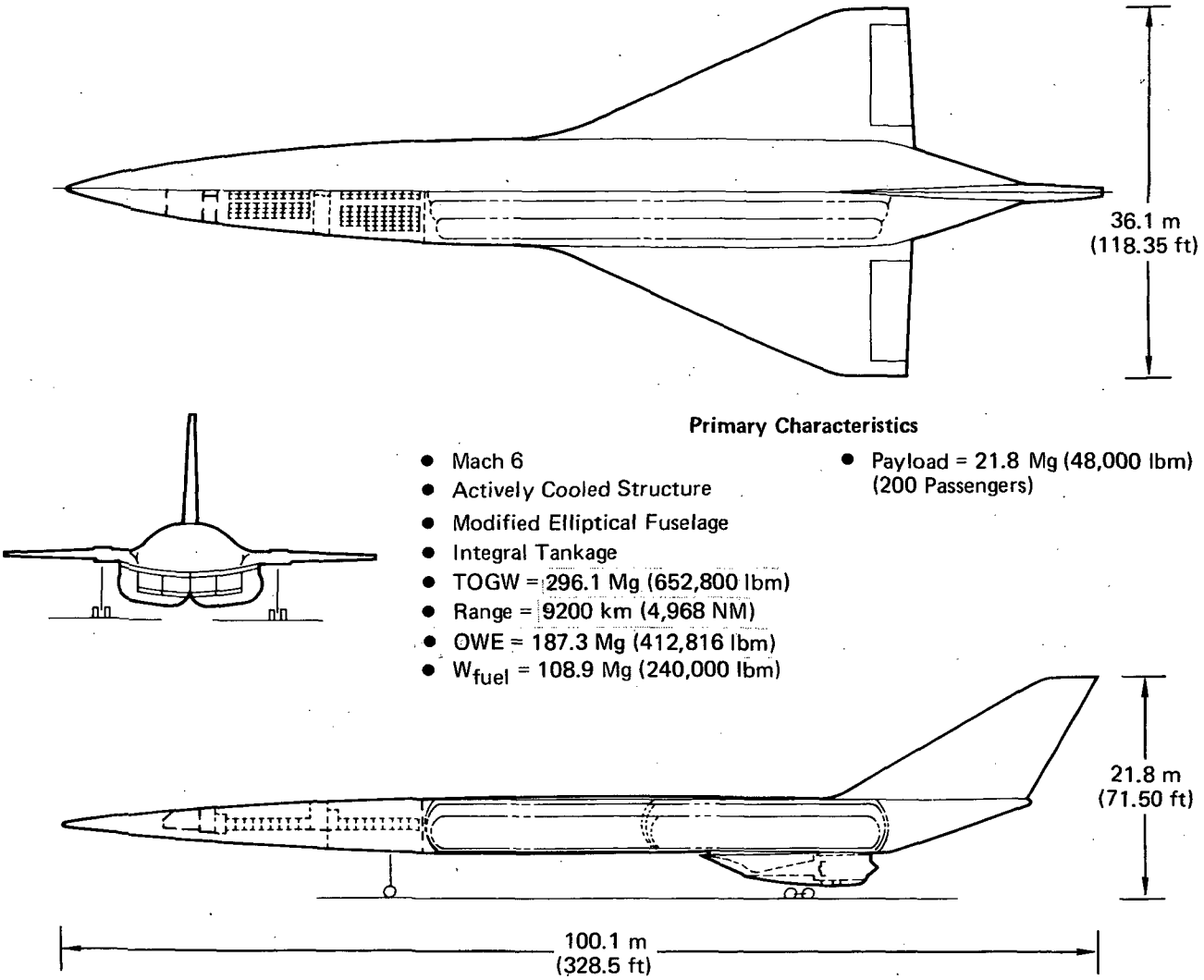

FIGURE 1
BASELINE AIRCRAFT

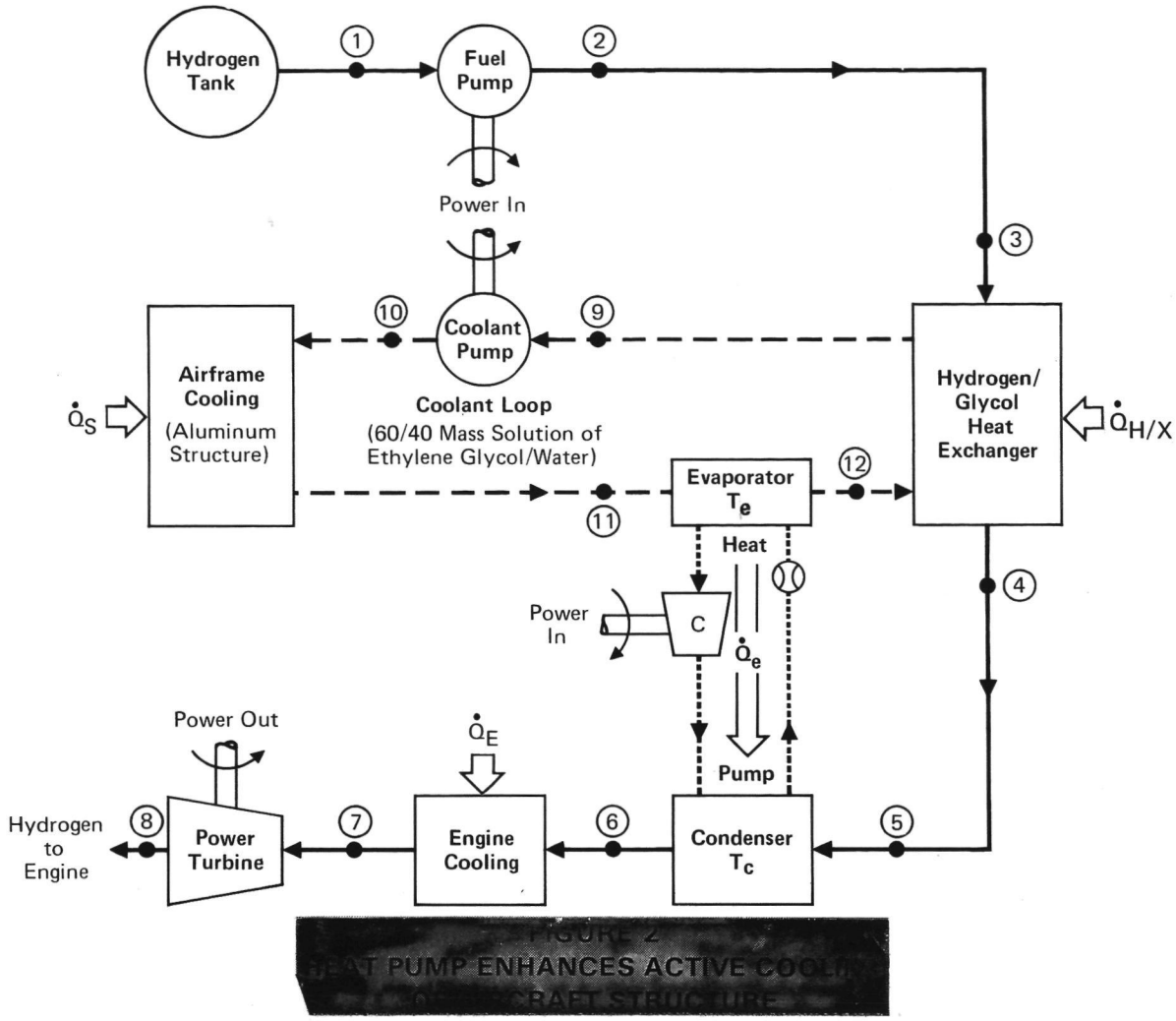

FIGURE 2
HEAT PUMP ENHANCES ACTIVE COOLING OF AIRCRAFT STRUCTURE

Study results show that sufficient power can be extracted from the hydrogen fuel to drive the heat pump and aircraft subsystems. An assessment of various heat pump/power extraction arrangements resulted in selection of a multi-pass condenser design, where power is extracted from the hydrogen fuel prior to a subsequent pass through the condenser. This design limits hydrogen outlet and hence the condenser temperature to a level consistent with efficient heat pump performance and permits the use of a conventional refrigerant such as Freon R-11. Study results demonstrate that with the aid of a heat pump it is technically feasible to cool to aluminum temperatures the airframe structure of an unshielded Mach 6 aircraft. Although the use of a heat pump (in lieu of external shielding) increases the mass of the baseline aircraft, spinoff benefits in specific impulse and drag

offset the mass gain such that a small net improvement in aircraft performance is realized.

INTRODUCTION

Numerous studies (references 1, 3, 4, and 5) conducted during the past several years have assessed the potential benefits of using the hydrogen fuel as a heat sink to cool Mach 6 aircraft structure. Cooling to aluminum temperatures is of particular interest due to the materials availability, high structural efficiency, and known long-life fabrication characteristics. However, due to the low operating temperature of aluminum, the allowable temperature rise of the hydrogen fuel (and hence its capacity for structural cooling) is severely restricted. In the past, a portion of the aircraft was shielded to reduce structural cooling requirements to a level compatible with the achieveable hydrogen heat sink. A potential alternate solution, investigated during the present program, uses a large capacity heat pump to increase the amount of hydrogen heat sink available for structural cooling. The design philosophy is illustrated by the heat pump/fuel system arrangement presented in figure 2. As shown, the airframe heat load is absorbed and transported by the glycol/water coolant and rejected to the hydrogen fuel. A portion of the load is rejected directly, via the heat exchanger, raising the temperature of the hydrogen to the value of T_4. Additional heat sink capacity for structural cooling is achieved by using a heat pump to reject heat at higher fuel temperatures, achieving a hydrogen temperature of T_6.

This program was designed to establish concept feasibility, evaluate advantages or disadvantages relative to the baseline shielded aircraft, and determine the cooling capability of the heat pump concept relative to cooling needs of a bare aluminum aircraft. Three heat pump/fuel system arrangements were analyzed in selecting a preferred concept. Also, detailed schematics of the fuel/coolant system were derived for the baseline aircraft, a bare aluminum heat pump configured aircraft, and an advanced aircraft with a 25% improvement in lift-to-drag ratio. Power extraction, heat pump, fuel system, auxiliary power system, and

coolant system components were sized and the resultant mass of the heat pump configured aircraft compared to the baseline. In addition to aircraft mass comparisons, drag and specific impulse adjustments were determined and used in computing aircraft performance.

Study results and conclusions are discussed in the body of the report; analysis methods used are presented in the Appendix.

LIST OF SYMBOLS

ACS	Active cooling system
APS	Auxiliary power system
Btu	British thermal units
C	Compressor
C_D	Drag coefficient
C_L	Lift coefficient
C_P	Material specific heat, J/kg.K (Btu/lbm °F)
COP	Coefficient-of-performance
D	Diameter
D_S	Specific diameter
F	Pumping power conversion factor, g/kW.s (lbm fuel/HP-hr)
H	Adiabatic head, m (ft)
HP or hp	Horsepower
h	Enthalpy, J/g (Btu/lbm)
Hr	Hour
in.	Inch
J	Mechanical equivalent of heat
L	Length, cm (in.)
L/D	Lift-to-drag ratio
lbf	Pound force
lbm	Pound mass
M	Mach
MCAIR	McDonnell Aircraft Company
$\dot{m}$	Mass flow rate, kg/s (lbm/sec)
N	Rotational speed
N_s	Specific speed
n	Number of stages
OWE	Operational weight empty, Mg (lbm)
psi	Pounds force per square inch
P	Pressure, Pa (psi), Tube pitch, cm (in.)
PR	Pressure ratio
Q	Volumetric flow, m^3/s (ft^3/sec)
$\dot{Q}$	Heating or cooling load, W (Btu/sec)

LIST OF SYMBOLS (Continued)

q	Dynamic pressure, Pa (lbf/ft^2)
$\dot{q}$	Heat flux, kW/m^2 (Btu/ft^2 sec)
R	Universal gas constant
Re	Reynolds number
T	Temperature, K (°F)
TOGW	Takeoff gross weight, Mg (lbm)
TPS	Thermal protection system
V	Velocity, m/s (ft/sec)
W	Power, MW (HP)
α	Angle-of-attack, deg
γ	Ratio of specific heats
δ	Delta; difference
ε	Heat exchanger effectiveness
η	Adiabatic efficiency
θ	Time[illegible]
μ	Fluid viscosity, Pa·s (lbm/ft sec)
ρ	Density, kg/m^3 (lbm/ft^3)
T	Turbine

SUBSCRIPTS

1	Inlet
2	Exit
c	Coolant, condenser, compressor
e	Evaporator
E	Engine
F	Freon
f	Fuel
H/X	Heat exchanger
H_2	Hydrogen
P	Pump
S	Structure (Airframe)
st	Stage
T	Tip
t	Turbine
MAX	Maximum

BASELINE AIRCRAFT CHARACTERISTICS

The reference 1 Mach 6 transport presented in figure 1 serves as the basis for conducting this program. As shown, the baseline aircraft is actively cooled, employing thermal shielding (external TPS) to reduce the aerodynamic heat load to a level that is compatible with the amount of hydrogen fuel heat sink available for structural cooling. The aircraft is sized to carry 200 passengers (21.77 Mg; 48,000 lbm payload) a distance of 9200 km (4968 NM).

Pertinent aerodynamic, thermodynamic, and propulsive characteristics for the baseline aircraft are summarized in table 1. As shown, the baseline airframe heat load (shielded aircraft) is approximately 52% of that experienced by a bare aluminum aircraft. Engine cooling requirements and fuel system pressures used throughout the study are for a Mach 6 Airframe-Integrated Scramjet as presented in references 2 and 6. The maximum allowable hydrogen fuel temperature (1144 K; 2060 °R) was selected based on results of the reference 3 study.

A schematic noting operating characteristics of the fuel/coolant system for the baseline aircraft is presented in figure 3. As shown, the hydrogen fuel is heated to 699 K (1258 °R) in satisfying airframe, subsystem, and engine cooling requirements. Since this represents only approximately 60% of the maximum allowable temperature rise of the hydrogen fuel, the potential for additional cooling and hence the possibility of reducing thermal shielding requirements is established. Power to drive aircraft subsystems is supplied by a liquid hydrogen/oxygen burning auxiliary power system (APS).

TABLE I
AIRCRAFT CHARACTERISTICS

Study Elements	Characteristics
1. Baseline Aircraft	• Mach 6 Hydrogen Fueled Transport • TOGW = 296.1 Mg (652,800 lbm) • Range = 9,200 km (4,968 NM)
2. Design Point	• Mach 6 Cruise at 31.4 km (103,500 ft) • Dynamic Pressure = 23.9 kPa (500 psf) • Cruise L/D = 4.66
3. Airframe Cooling	• 2,985 m^2 (32,134 ft^2) of Actively Cooled Aluminum Structure at an Average Temperature of 367 K (200°F) • 5.85 Mg (12,900 lbm) of Shielding (External TPS) • *Airframe Heat Load, $\dot{Q}_s$ = 47.4 MW (4.5×10^4 Btu/sec) . . . . 52% of Airframe Heat Load Experienced by Bare Aluminum Aircraft
4. Engine Cooling	• $\dot{Q}_E$ = 84.7 MW (8.03×10^4 Btu/sec) • Engine Fuel Flow Rate, $\dot{m}_f$ = 13.6 k g/s (30 lbm/sec)
5. Fuel System Pressures	• 4.83 MPa (700 psia) Minimum at Engine Fuel Injectors • Total Pressure Drop of 2.07 MPa (300 psi) . . . . 0.34 MPa (50 psi) Drop in Fuel System and 1.72 MPa (250 psi) Drop in Engine Cooling Circuit.
6. Hydrogen Fuel	• Tank Conditions T = 21 K (37°R) P = 0.14 MPa (20 psia) • Maximum Allowable Temperature of 1,144 K (2,060°R)

*Airframe heat load matched to hydrogen fuel available for structural cooling (see page 65 of Reference 1).

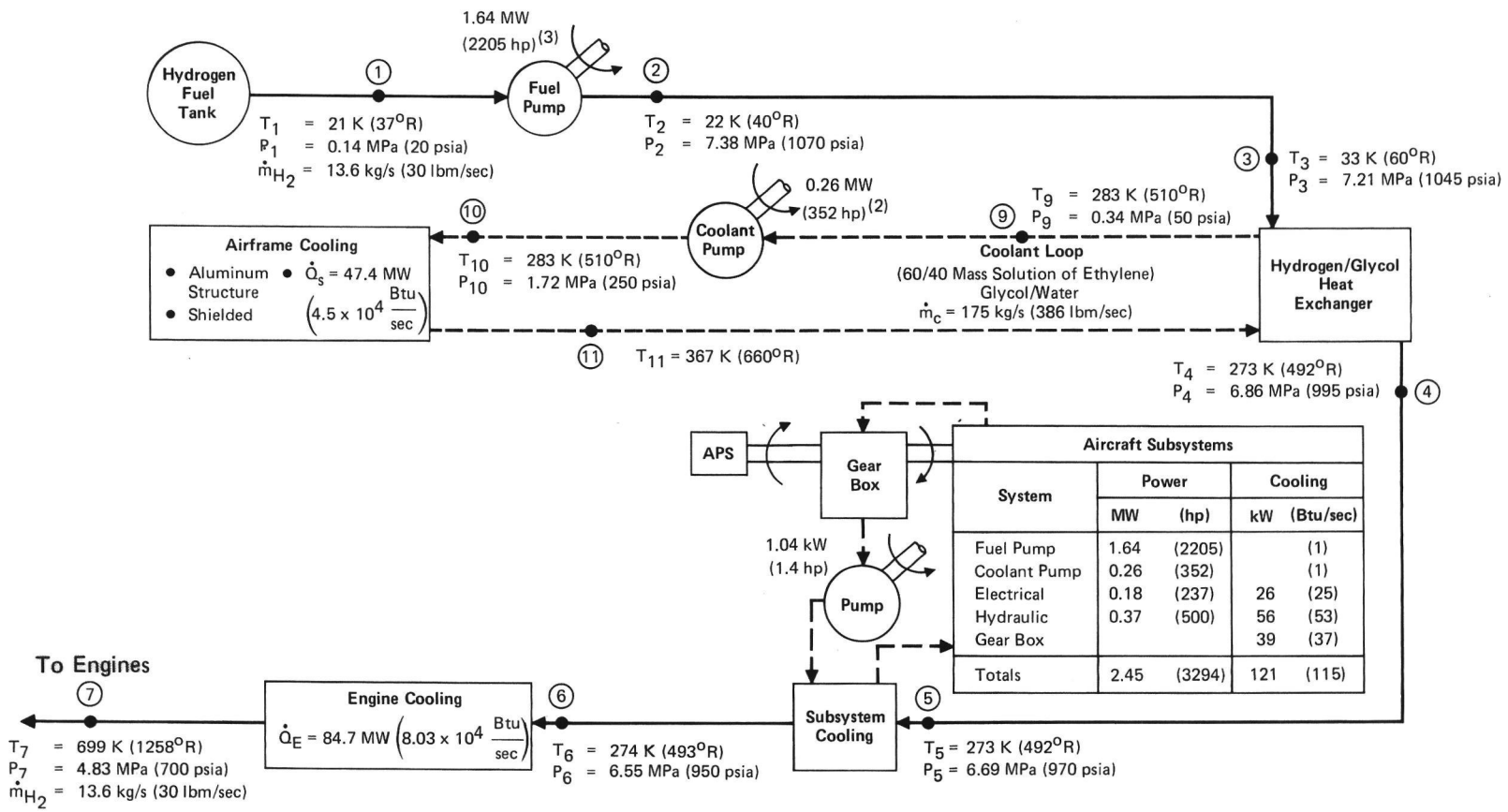

System	Power MW	Power (hp)	Cooling kW	Cooling (Btu/sec)
Fuel Pump	1.64	(2205)		(1)
Coolant Pump	0.26	(352)		(1)
Electrical	0.18	(237)	26	(25)
Hydraulic	0.37	(500)	56	(53)
Gear Box			39	(37)
Totals	2.45	(3294)	121	(115)

Notes:
1. Cooled by fluid being pumped
2. Coolant density = 1.08 Mg/m^3 (67.6 lbm/ft^3)
3. Hydrogen density = 70.5 kg/m^3 (4.4 lbm/ft^3)

FIGURE 3

SCHEMATIC OF FUEL/COOLANT SYSTEM FOR MACH 6 BASELINE AIRCRAFT
L/D = 4.66

POWER EXTRACTION

Analyses were performed to determine the amount of shaft power that could be extracted from the baseline aircraft's hydrogen fuel system to be used in driving a large capacity heat pump. Analyses were performed assuming power extraction both upstream (Option A) and downstream (Option B) of the engine cooling circuit as illustrated in figure 4. At the upstream location (Option A) the hydrogen fuel is at a relatively low energy state (T_5 = 273K; 492°R) and for a given power output requires a large pressure drop across the turbine, and high fuel pressures. The excess power (turbine output minus fuel and coolant pump requirements) available at this location increases with increasing fuel pressure up to a maximum of 8.4 MW (11,200 HP) at a fuel pressure of 34.5 MPa (5000 psia). At higher fuel pressures, the excess power available to drive a heat pump decreases because the increment in fuel pump requirements now exceeds the increment in power turbine output.

Figure 4 also shows that, for the same fuel pressure, four to six times as much excess power is available by extracting downstream (Option B) rather than upstream (Option A) of the engine cooling circuit. Extracting power downstream of the engine cooling circuit was therefore selected as the preferred option to ensure an adequate power supply for driving the heat pump, and to minimize fuel pressures.

Characteristics of a representative hydrogen turbine with a power output of 22.4 MW (30,000 HP) are presented in table 2. Turbine characteristics were determined (see Appendix) with the aid of references 7 through 9.

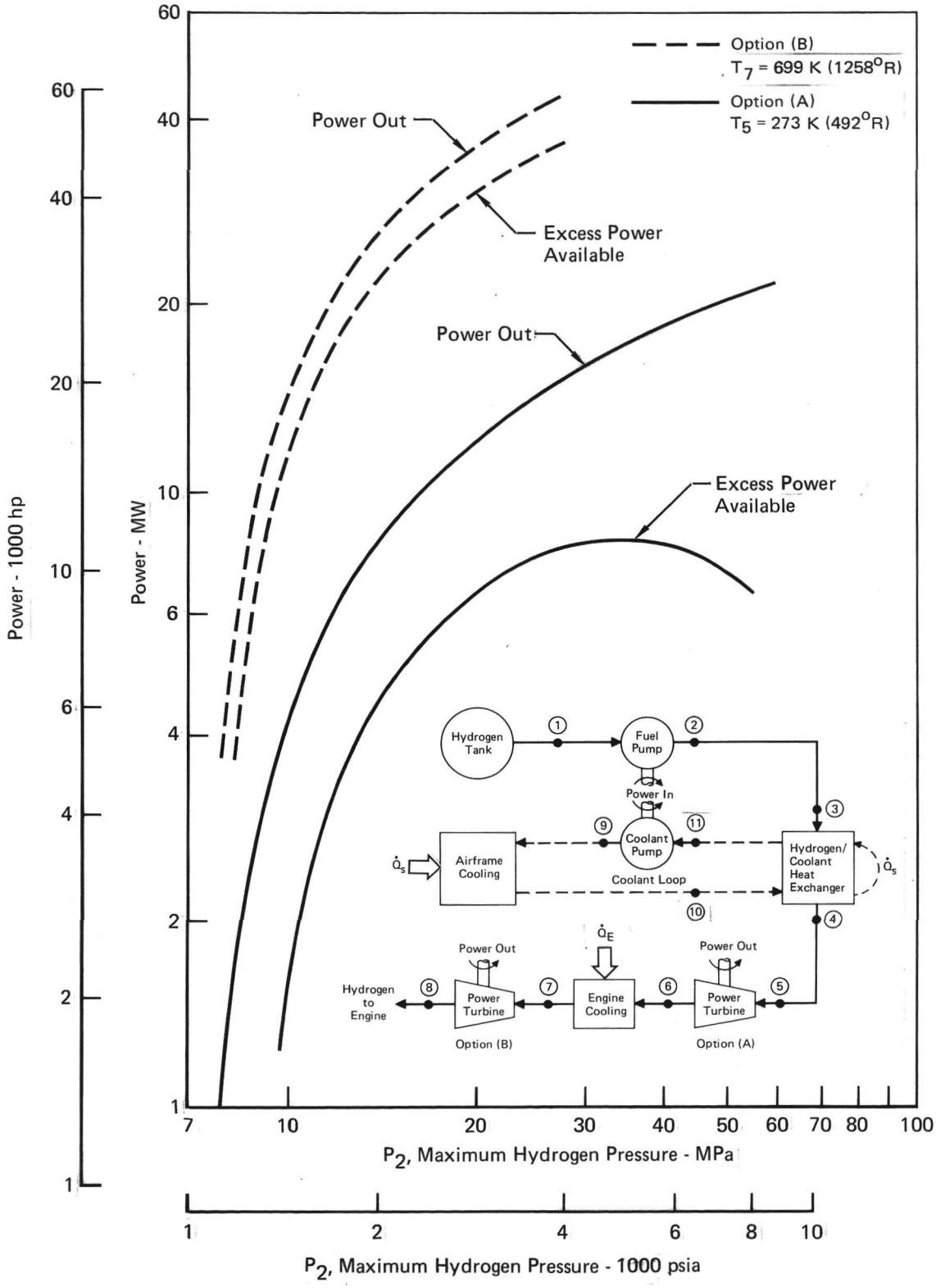

FIGURE 4

POWER TURBINE OUTPUT ... HYDROGEN FUEL PRESSURE FOR ... BASELINE AIRCRAFT

TABLE 2

CHARACTERISTICS OF A 22.4 MW (30,000 HP) HYDROGEN POWER TURBINE

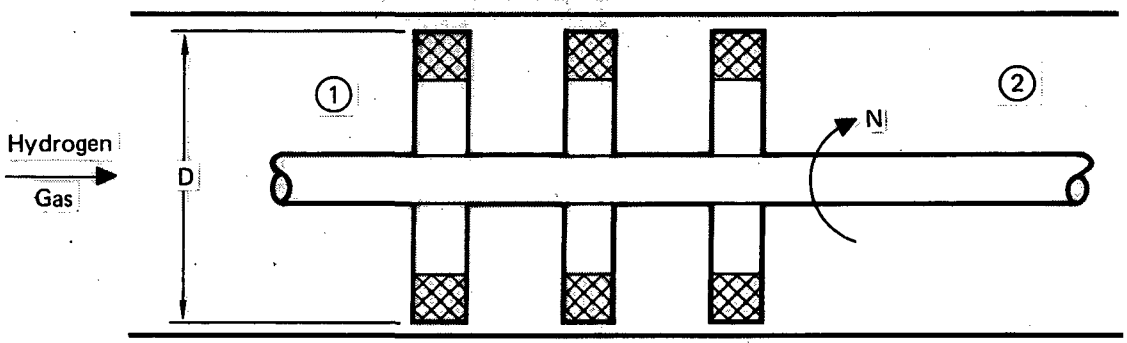

Flow Conditions

- $\dot{m}_{H_2}$ = 13.6 kg/s (30 lbm/sec)
- PR = 2.43
- P_1 = 11.72 MPa (1700 PSIA)
- T_1 = 722 K (1300°R)
- P_2 = 4.83 MPa (700 PSIA)
- T_2 = 610 K (1098°R)

Turbine Characteristics

- Turbine Type ..... Axial
- No. of Stages 3
- Power Output ..... 22.4 MW (30,000 hp)
- Wheel Diameter, D ..... 48.5 cm (19.1 in.)
- Turbine Speed, N ..... (24,000 rpm)
- Tip Speed, V_T ..... 610 m/s (2000 ft/sec)
- Weight (Turbine Assembly) ..... 200 kg (440 lbm)
- Volume (Turbine Assembly) ..... 0.15 m^3 (5.2 ft^3)

"Page missing from available version"

page 16

HEAT PUMP ANALYSES

Three heat pump concepts were evaluated and are discussed in the following sections.

Concept 1 - A schematic and analysis results for the Concept 1 heat pump/fuel system arrangement are presented in table 3. This concept employs a cascaded heat pump driven by a power turbine located downstream of the engine cooling circuit. As shown, the approach significantly enhances active cooling capability but is limited to an airframe heat load equal to approximately 85% of that experienced by a bare aluminum aircraft. Increasing the heat load beyond the 85% limit would exceed the maximum allowable fuel temperature of 1144K (2060°R) and result in overheating of the engine (see reference 3). At the limiting condition, nine stages of cascading are required to pump heat from an evaporator temperature of 328K (590°R) to a condenser temperature of 731K (1315°R), a spread of some 403K (725°R). Due to the high refrigeration cycle temperatures, the last three stages require an exotic refrigerant such as mercury. Cascading requirements were based on the recommendations of reference 10, namely, a maximum evaporator to condenser temperature spread of 56K (100°R) per stage and a 11K (20°R) temperature difference for heat transfer between stages. The large increase in condenser temperature with increasing heat load reduces the coefficient-of-performance (COP) and results in a dramatic increase in heat pump power requirements and condenser load.

Although it was recognized that maximum hydrogen fuel temperature could be lowered (extending the present operating limit) by extracting power upstream of the engine cooling circuit, this approach was not pursued. Concept 1 was eliminated from further consideration because of the extremely complex heat pump that would be required (nine or more stages of cascading, exotic refrigerants, and large power demands).

Concept 2 - The shortcomings of Concept 1 are directly traceable to the large increase in the temperature of the hydrogen as it passes through the condenser, resulting in high hydrogen

TABLE 3

CONCEPT 1 HEAT PUMP/FUEL SYSTEM CHARACTERISTICS

$\dot{Q}_s$ Airframe Heat Load (% of $\dot{Q}_{s_o}$)	Heat Pump Characteristics										T_7 - Maximum Hydrogen Temperature	
	Coeff of Perf	Number of Stages	Temperatures				Load - % of $\dot{Q}_s$		Power			
			Evaporator		Condenser		Evaporator	Condenser	MW	HP		
			(K)	(^oR)	(K)	(^oR)					(K)	(^oR)
70	7.25	1	344	619	368	662	14	16	1.2	1,600	782	1,407
76	1.81	2	337	607	430	774	22	34	8.4	11,200	844	1,519
81	0.69	5	331	596	570	1,026	29	71	30.9	41,500	984	1,771
85	0.41	9	328	590	731	1,315	33	115	62.6	83,900	1,144	2,060

Notes:
1. $\dot{Q}_s$, airframe heat load
2. $\dot{Q}_{s_o}$, airframe heat load for bare aluminum aircraft equal to 90.7 MW (8.6×10^4 Btu/sec)
3. Number of cascading stages based on an evaporator to condenser spread of 56 K (100°R) per stage and a 11 K (20°R) temperature difference for heat transfer between stages.
4. Concept limited by maximum allowable hydrogen temperature of 1144 K (2,060°R)

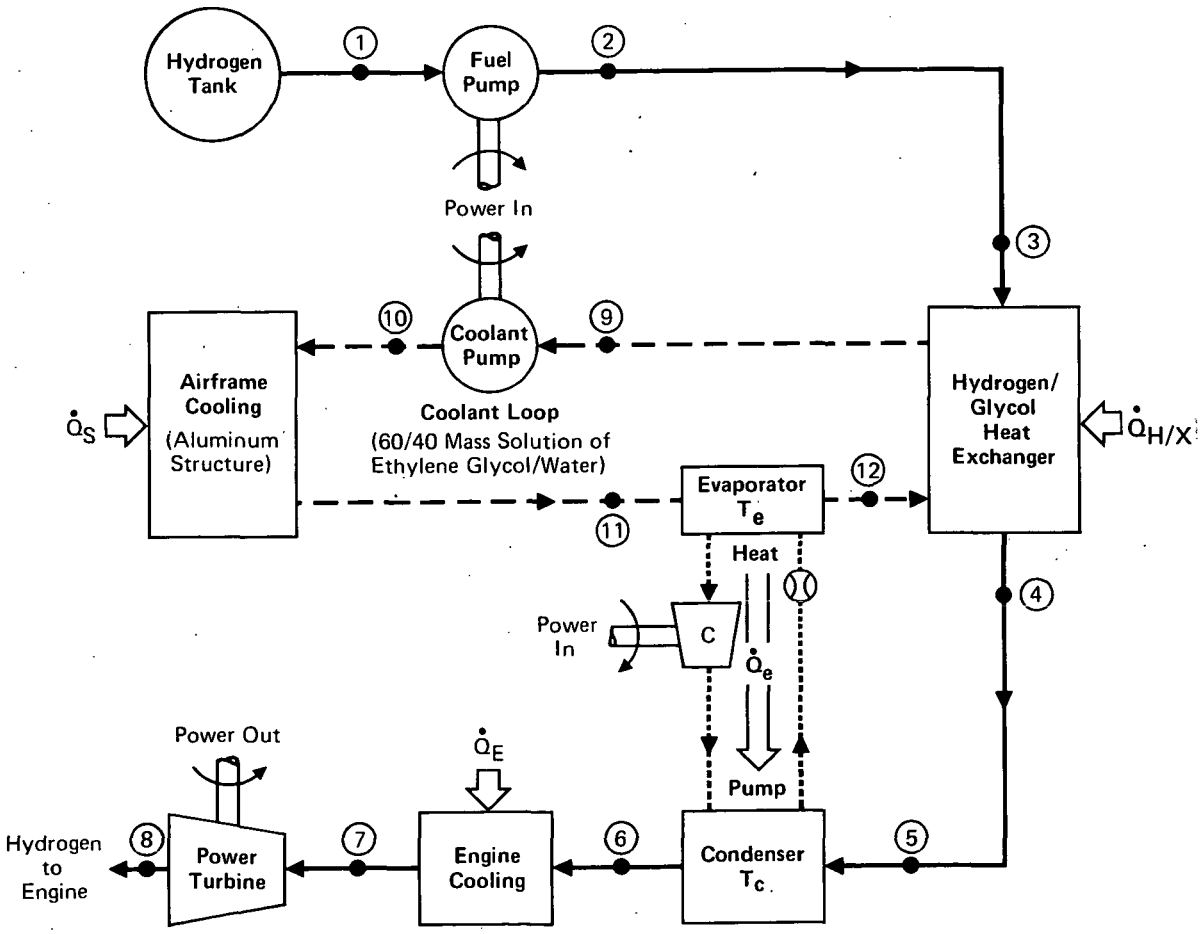

outlet temperatures and hence, high condenser temperatures (condenser temperature is equal to hydrogen outlet temperature plus 11K; 20°R). These shortcomings can be circumvented by a multi-pass condenser as illustrated in table 4. With this approach, power is extracted from the hydrogen fuel stream, lowering its temperature between passes through the condenser, thereby limiting hydrogen outlet and condenser temperatures.

Concept 2 heat pump/fuel system characteristics as a function of coefficient-of-performance are tabulated in table 4. Note that this concept can absorb 100% of the bare aluminum aircraft's airframe heat load. As shown in the table and in figure 5, the heat pump must be sized to operate at a coefficient-of-performance of 1.17 (condenser temperature of 454K; 817°R), such that the power extracted equals the amount of power required to drive the heat pump, fuel pump, and aircraft subsystems. At this condition some 43.6 MW (58,500 HP) of mechanical energy is extracted from the hydrogen fuel system (48% of airframe heat load), requiring a maximum fuel pressure of 35.6 MPa (5160 psia) to satisfy the design condition of a 4.8 MPa (700 psia) minimum pressure at the engine fuel injectors. As shown in table 4, a three stage cascaded heat pump is proposed to span the 136K (244°R) spread between evaporator and condenser temperatures.

Selected Concept - As shown previously (table 4), Concept 2 is constrained to operate at a coefficient-of-performance of 1.17, as operation at a higher COP results in power extraction rates that are in excess of requirements. The selected concept (figure 6) permits operation at a higher coefficient-of-performance by utilizing the excess power to drive a hydrogen compressor downstream of the condenser. Operating at a higher coefficient-of-performance lowers the condenser temperature and reduces the size, complexity (cascades), and power requirements of the heat pump. Adding the hydrogen compressor reduces maximum fuel pressures by approximately a factor of 2 which reduces fuel pump

TABLE 4 (a)

HEAT PUMP WITH MULTIPASS CONDENSER AND POWER EXTRACTION COOLS MACH 6 BARE ALUMINUM AIRCRAFT

(SI Units)

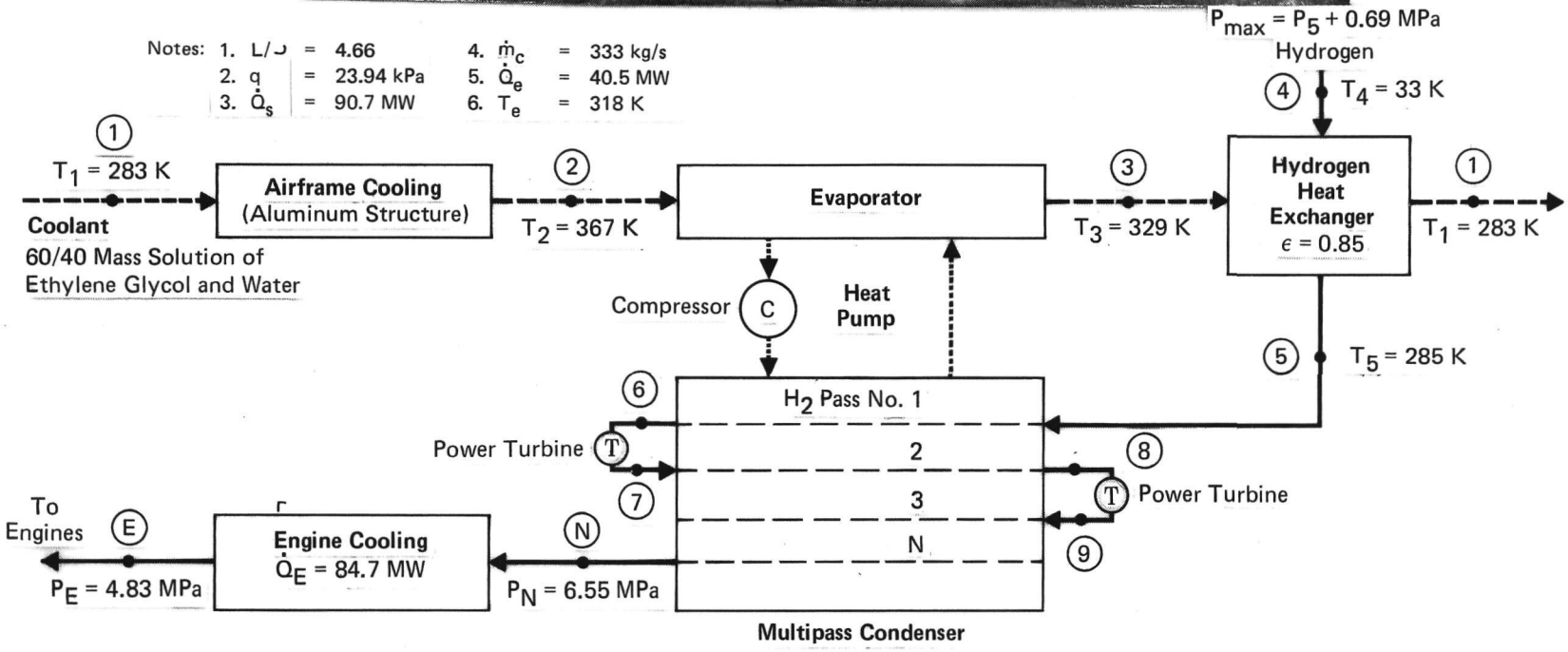

Heat Pump Characteristics						Hydrogen Conditions			Power Characteristics - MW						
									Required				Extracted		
Cop	Number of Stages	$\dot{Q}_c$ (MW)	H_2 Passes	T_c (K)	$T_c - T_e$ (K)	T_N (K)	T_E (K)	P_{max} MPa	Heat Pump	Fuel Pump	Aircraft Subsys	Total	No. of Turbines and PR	Total	Excess
2.865	1	54.8	4	374	56	363	788	39.4	14.1	8.3	1.5	23.9	3 at 1.81	39.1	15.2
2.5	1	56.9	4	382	64	371	796	38.6	16.2	8.2		25.9	3 at 1.80	39.6	13.7
2.0	2	61.2	3	398	79	387	812	40.3	20.3	8.5		30.3	2 at 2.46	40.5	10.2
2.0	2	61.2	4	398	79	387	812	37.3	20.3	7.9		29.7	3 at 1.78	40.5	10.8
1.5	2	67.5	3	424	106	413	838	37.8	27.0	8.0		36.5	2 at 2.38	41.9	5.4
1.17	3		3	454	136		868	35.6					2 at 2.31	43.6	0
1.0	3	81.2	3	478	159	467	892	34.2	40.5	7.2		49.2	2 at 2.26	44.8	–4.4
0.5	7	121.3	2	637	318	626	1051	33.8	81.0	5.3		87.8	1 at 5.1	53.6	–34.2

TABLE 4 ( )

HEAT PUMP WITH MULTIPASS CONDENSER AND POWER EXTRACTION COOLS MACH 6 BARE ALUMINUM AIRCRAFT

(Customary Units)

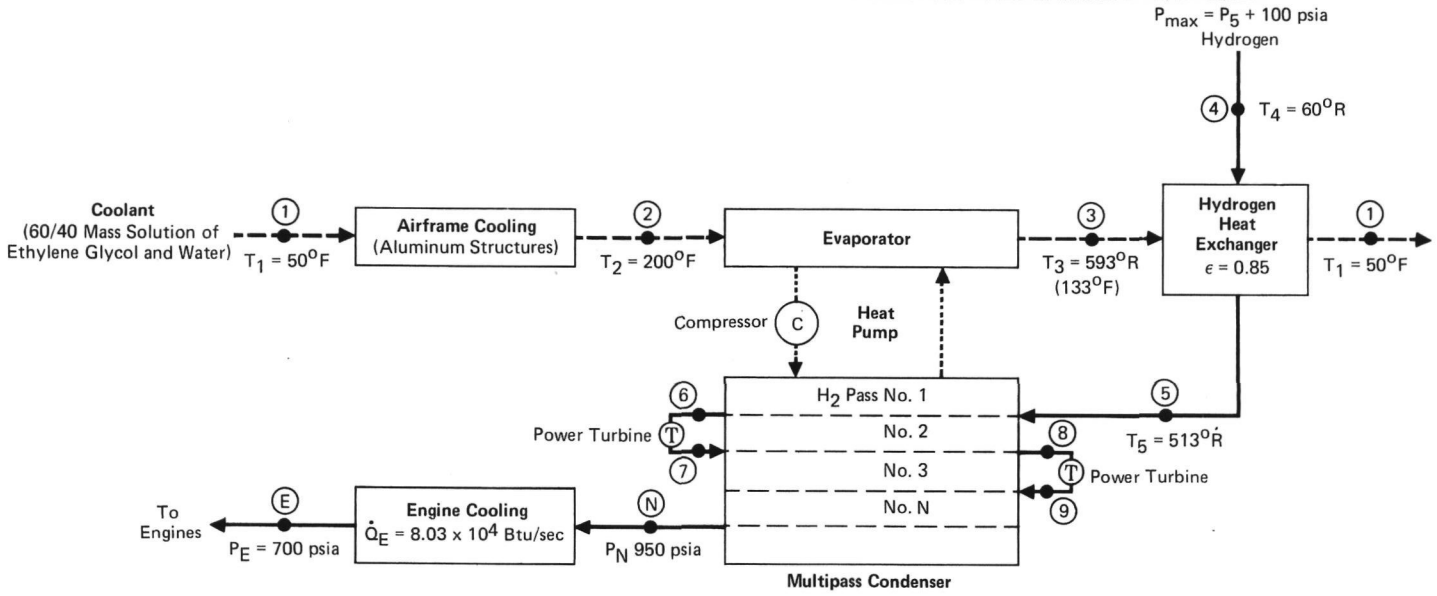

Notes:
1. L/D = 4.66
2. q = 500 psf
3. $\dot{Q}_s = 8.6 \times 10^4$ Btu/sec
4. $\dot{m}_c = 735$ lb/sec ($T_i = 50^oF$, $T_o = 200^oF$)
5. $\dot{Q}_e = 3.84 \times 10^4$ Btu/sec (11,520 tons)
6. $T_e = 573\ ^oR$ (113^oF)

Heat Pump Characteristics								Hydrogen Conditions					Power Characteristics - hp						
COP	Number of Stages	$\dot{Q}_c$ (Btu/sec)	H_2 Passes	T_c, Cond Temp (^oR)	T_c, Cond Temp (^oF)	T_c-T_e (^oR)	Power* (hp/Ton)	T_N (^oR)	T_N (^oF)	T_E (^oR)	T_E (^oF)	P_{max} (psia)	Required: Heat Pump	Required: Fuel Pump	Required: Aircraft Subsystem	Required: Total	Extracted: No. of Turbines and PR	Extracted: Total	Excess
2.865	1	5.2×10^4	4	673	213	100	2.6	653	193	1,418	958	5,710	18,955	11,173	2,000	32,128	3 at 1.81	52,475	20,347
2.5	1	5.4×10^4	4	688	228	115	2.8	668	208	1,433	973	5,594	21,727	10,945		34,672	3 at 1.80	53,069	18,397
2.0	2	5.8×10^4	3	716	256	143	3.4	696	236	1,461	1,001	5,852	27,159	11,452		40,611	2 at 2.46	54,360	13,749
2.0	2	5.8×10^4	4	716	256	143	3.3	696	236	1,461	1,001	5,414	27,159	10,592		39,751	3 at 1.78	54,360	14,609
1.5	2	6.4×10^4	3	764	304	191	4.1	744	284	1,509	1,049	5,482	36,212	10,726		48,938	2 at 2.38	56,218	7,280
1.17	3		3	817	357	244				1,563	1,103	5,160					2 at 2.31	58,500	0
1.0	3	7.7×10^4	3	860	400	287	5.6	840	380	1,605	1,145	4,963	54,319	9,706		66,025	2 at 2.26	60,141	−5,884
0.5	7	11.5×10^4	2	1146	686	573	10.3	1,126	666	1,891	1,431	4,909	108,637	9,601		120,238	1 at 5.1	71,887	−48,351

*Power required to drive heat pump and fuel pump divided by evaporator load.

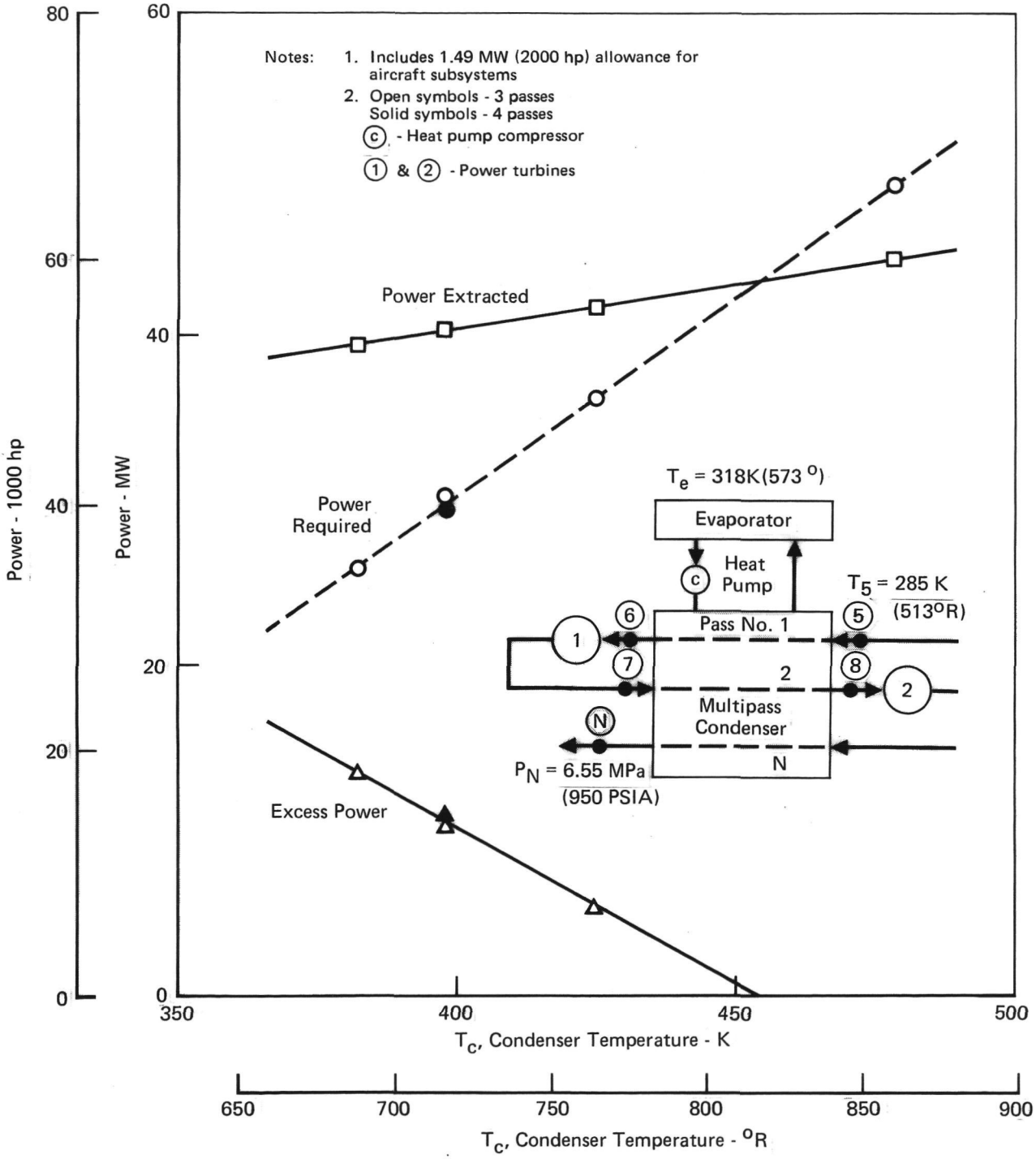

FIGURE 5

POWER CHARACTERISTICS - HEAT PUMP WITH MULTIPASS CONDENSER COOLS MACH 6 BARE ALUMINUM AIRCRAFT

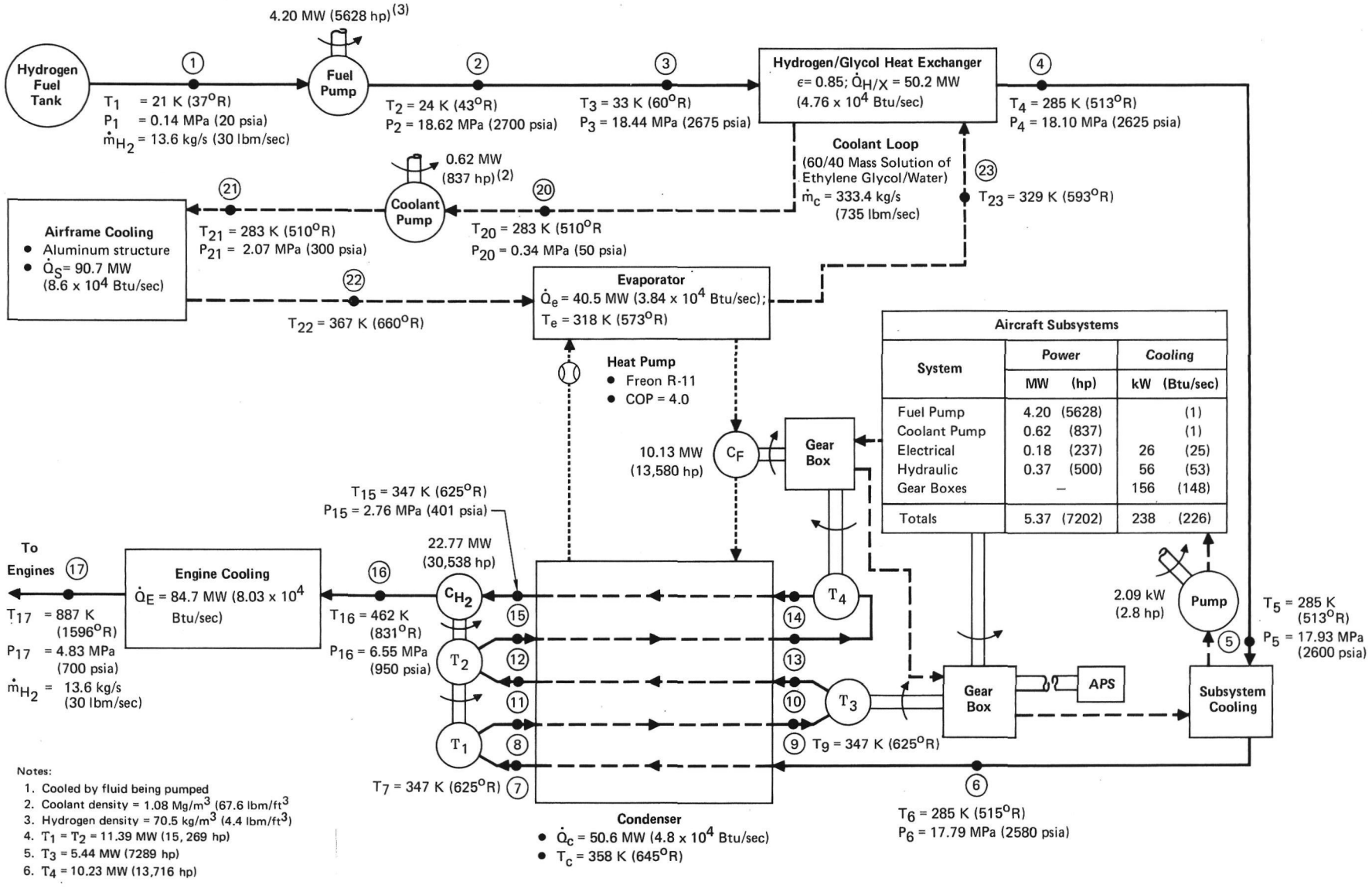

Notes:

1. Cooled by fluid being pumped
2. Coolant density = 1.08 Mg/m^3 (67.6 lbm/ft^3)
3. Hydrogen density = 70.5 kg/m^3 (4.4 lbm/ft^3)
4. $T_1 = T_2 = 11.39$ MW (15, 269 hp)
5. $T_3 = 5.44$ MW (7289 hp)
6. $T_4 = 10.23$ MW (13,716 hp)

FIGURE 6
SELECTED HEAT PUMP/FUEL SYSTEM ARRANGEMENT FOR MACH 6 BARE ALUMINUM AIRCRAFT (L/D =4.66)

requirements, and fuel system and heat exchanger mass. Since the present system has no known upper limit on the COP, selection of an optimum value would require performing a detailed trade study to identify a minimum mass or minimum cost system; such a study was beyond the scope of the present program. For the selected COP of 4, a single stage heat pump and a conventional refrigerant, Freon R-11, can be used. (This COP was selected as a reasonable compromise between further decreasing heat pump requirements and increasing the number of hydrogen passes through the condenser.) As shown in figure 6, the selected concept requires five passes through the condenser and four power turbines. Two turbines connected in tandem drive the hydrogen compressor, another provides power for aircraft subsystems, and the fourth drives the heat pump.

The results of figure 6 demonstrate the technical feasibility of using a large capacity heat pump to actively cool the aluminum structure of an unshielded Mach 6 transport. Results of a component sizing and mass analysis are presented in the section which follows. An assessment of the heat pump concept versus external shielding and the resultant impact on aircraft performance is discussed in a later section.

Heat Pump Sizing - Following the procedure of reference 10 (see Appendix), cycle characteristics of the heat pump were determined, establishing system pressures and the refrigerant mass flow rate required to absorb the evaporator load. For the figure 6 heat pump which operates with Freon R-11 with a compression efficiency of 60%, a refrigerant mass flow rate of 285.5 kg/s (629.5 lbm/sec) is required to absorb the evaporator load of 40.5 MW (11,520 tons of cooling). The system operates between an evaporator temperature of 318K (573°R) and a condenser temperature of 358K (645°R), with corresponding pressures of 0.19 MPa (27.5 psia) and 0.59 MPa (85 psia), respectively.

Based on the above operating conditions, heat pump components were sized and mass and volume requirements were determined and are presented in table 5. As shown, the mass and vol-

ume of the heat pump system is 10.46 Mg (23,050 lbm) and 11.77 m^3 (416 ft^3), respectively.

TABLE 5
COMPONENT MASS AND VOLUME BREAKDOWN FOR SELECTED HEAT PUMP SYSTEM*

Component	Mass		Volume	
	Mg	lbm	m^3	ft^3
1. Evaporator (Dry)	2.90	6,400	3.57	126
2. Condenser (Dry)	3.36	7,400	5.86	207
3. Freon Compressor	0.89	1,950	1.27	45
4. Compressor Drive Turbine & Gear Box	0.18	400	0.11	4
5. Freon	2.27	5,000	–	–
6. Lines & Controls (5% of 1-3)	0.36	800	0.54	19
Subtotal (Heat Pump)	9.96	21,950	11.35	401
7. Hydrogen Compressor & Drive Turbines (2)	0.50	1,100	0.42	15
Total Heat Pump System	10.46	23,050	11.77	416

*See Figure 6

System Impact - The mass of the fuel/coolant system for the heat pump configured, bare aluminum aircraft (figure 6), and the baseline shielded aircraft (figure 3) have been determined and are compared in table 6. As shown, the bare aluminum aircraft realizes a mass reduction due to elimination of the external thermal protection system (TPS) and the savings in power generation propellant requirements. However, these mass savings are overpowered, primarily due to the mass of the heat pump system (10.46 Mg; 23,050 lbm), such that aircraft mass (relative to the baseline) is increased by 2.75 Mg (6050 lbm). The resultant impact on aircraft performance is discussed in a later section.

TABLE 6

Mass Element	Baseline Aircraft		Bare Aluminum Aircraft			
			Actual		Delta (1)	
	(Mg)	(lbm)	(Mg)	(lbm)	(Mg)	(lbm)
Shielding (External TPS)	5.85	12,900	0	0	−5.85	−12,900
Active Cooling System	4.31	9,500	5.40	11,900	1.09	2,400
Hydrogen Fuel Pump	0.05	100	0.11	250	0.07	150
Aircraft Power Generation System (2)	3.13	6,900	0.11	250	−3.02	−6,650
Heat Pump System	–	–	10.46	23,050	10.46	23,050
Total	13.34	29,400	16.08	35,450	2.75	6,050

(1) Delta; change relative to baseline

(2) Baseline aircraft: Mass of APS propellant consumed during cruise
Bare aluminum aircraft: Mass of power turbine and gear box

Even though subsystem power requirements for the bare aluminum aircraft are more than double those of the baseline (see figures 3 and 6), the mass of its power generation system is 3.02 Mg (6650 lbm) lighter. As noted in table 6, this mass savings is attributable to the method used in providing power to drive aircraft subsystems during cruise. That is, the baseline aircraft uses an auxiliary power system (APS) which consumes 3.13 Mg (6900 lbm) of propellant in satisfying subsystem power requirements, whereas the bare aluminum aircraft extracts power from the hydrogen fuel system and is charged only with the mass of the power turbine and gear box (0.11 Mg; 250 lbm). Although the reference 1 aircraft was retained as the baseline for the purpose of this study, it should be noted that mass and performance characteristics of this aircraft would be improved if re-configured with a hydrogen power turbine.

EFFECT OF IMPROVED AERODYNAMIC EFFICIENCY

Earlier work (reference 3) has shown that as aerodynamic efficiency (L/D) improves, the potential for active cooling of the structure decreases. This is due to the fact that as L/D increases the fuel heat sink available for cooling decreases at a faster rate than the aerodynamic heat load. Furthermore, since the baseline aircraft is a conceptual design, improvements in aerodynamic efficiency may be expected. Analyses were therefore performed to determine the effectiveness of the selected heat pump concept for an aircraft with a 25% improvement in L/D over the baseline aircraft.

Assuming that the 25% improvement in L/D is due to equal improvements in lift coefficient (C_L) and drag coefficient (C_D), it can be shown that for a fixed size aircraft of equal cruise mass and specific impulse (I_{sp}), the drag and hence the fuel flow rate, decreases by 20% whereas aerodynamic heat inputs decrease by only 8%. After adjusting the baseline fuel flow rate and engine and airframe cooling requirements, the selected heat pump concept was resized as summarized in figure 7. Note that even though the fuel heat sink available for cooling ($\dot{m}_{H_2}$) has been reduced 20%, the heat pump concept has adequate capacity to cool the unshielded Mach 6 aircraft to aluminum temperatures. Comparing figures 6 and 7, it can be observed that the major effects of a 25% improvement in L/D are, (a) a 78% increase in fuel pressure, (b) a 43% increase in fuel pump power requirements, (c) a 113K (204°R) increase in the maximum fuel temperature, and (d) the need for 5 rather than 4 power extraction turbines (20% increase in the amount of power extracted). Although increasing the L/D decreases airframe cooling requirements 8%, it can be noted from figures 6 and 7 that the heat pump evaporator load has increased by approximately 9%. This paradox is due to the large decrease in fuel flow rate which produces a corresponding decrease in the amount of heat that can be transferred directly to the fuel system via the hydrogen/

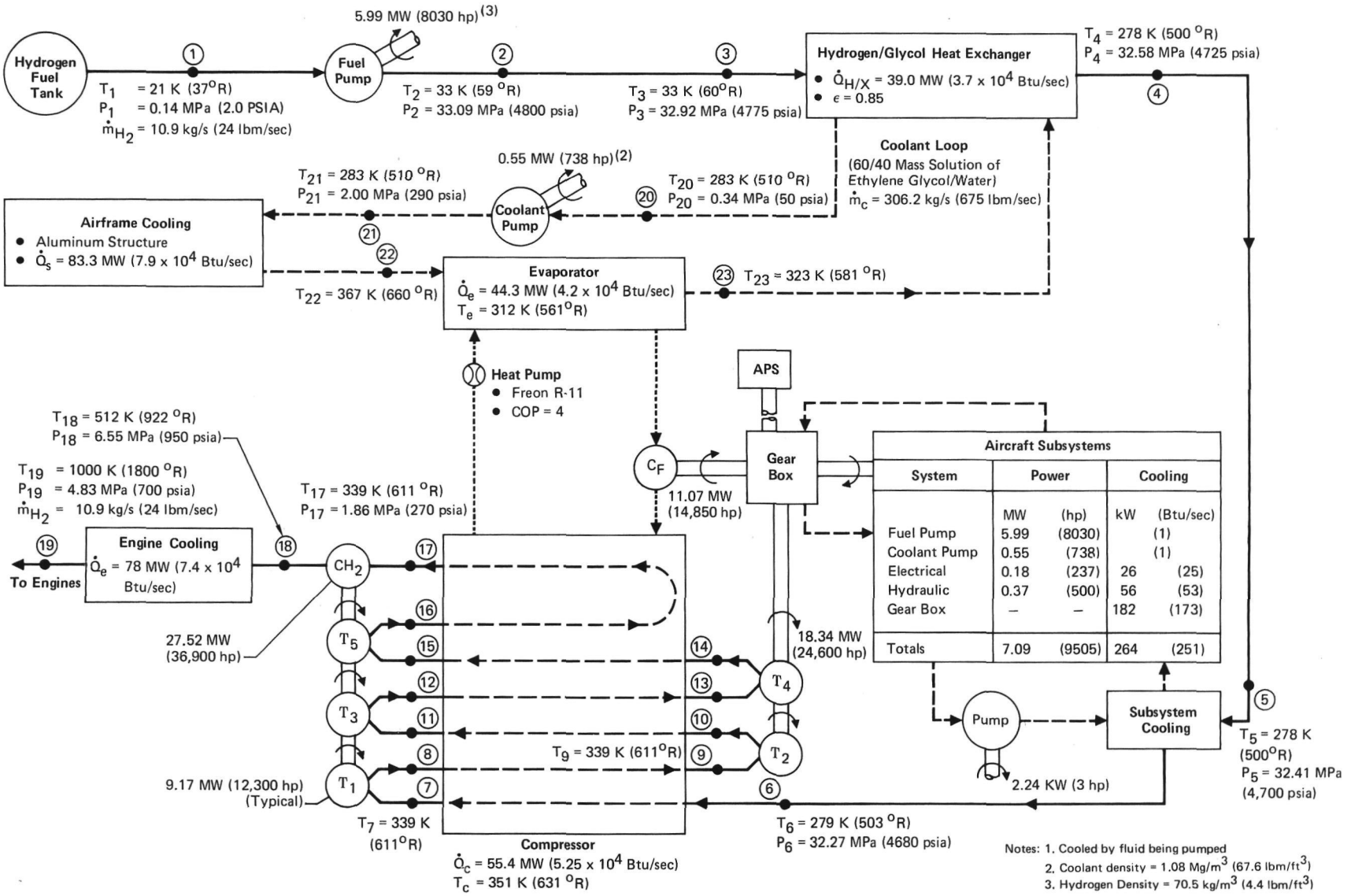

FIGURE 7

SCHEMATIC OF FUEL/COOLANT SYSTEM FOR MACH 6 BARE ALUMINUM AIRCRAFT WITH 25% IMPROVEMENT IN CRUISE L/D

glycol heat exchanger; the balance of the airframe heat load must be transferred by the heat pump.

For the purpose of this study it was assumed that the mass of the heat pump system would scale according to evaporator load. Hence, the mass of the heat pump for the aerodynamically improved aircraft was estimated to be 11.44 Mg (25,200 lbm), which is 9% more than the previously presented heat pump mass for the aircraft with an L/D = 4.66 (see table 5).

"Page missing from available version"

page 30

IMPACT ON AIRCRAFT PERFORMANCE AT L/D = 4.66 AND 5.83

Aircraft empty weight, payload, fuel requirements, and range for two heat pump configured bare aluminum aircraft are compared to the shielded baseline in table 7. As shown, the use of a heat pump in lieu of shielding increases aircraft empty weight (relative to the baseline) by 1.7% at an L/D of 4.66 and by 2.3% at an L/D of 5.83. The mass increase at an L/D = 5.83 would be reduced, relative to a shielded baseline operating at the same lift-to-drag ratio, as the present comparison does not account for the fact that additional shielding would be required at the higher L/D value to match airframe cooling requirements to the available hydrogen (fuel) heat sink.

Although the use of a heat pump (at L/D = 4.66) in lieu of shielding increases the mass of the baseline aircraft, spinoff benefits in drag and specific impulse (see table 8) offset the mass gain such that a small net improvement in performance is realized (see table 7). Note that these performance improvements occur singularly. That is, when the baseline range and fuel load are held constant, the payload is increased 2%. Likewise, by fixing the two remaining parameters, a 0.3% reduction in fuel requirements or a 0.4% increase in range can be achieved. In all cases aircraft take-off weight (TOGW) increases by approximately 1%.

Performance improvements (relative to the baseline) for the bare aluminum aircraft with an L/D of 5.83 range from an 8% fuel savings to a 67% increase in payload capability. Although these improvements are directly attributable to a 25% improvement in the baseline lift-to-drag ratio, the results are of interest to the present study since such improvements in aerodynamic efficiency may be more readily achieved with a bare aluminum aircraft than with a shielded aircraft.

TABLE 7

Mass Elements	Mass in Mg (lbm)				
	Baseline Aircraft L/D = 4.66	Bare Aluminum Aircraft			
		L/D = 4.66		L/D = 5.83	
		Actual	Delta(1)	Actual	Delta(1)
Aircraft Empty Weight(2)	165.47 (364,800)	168.21 (370,850)	1.7%	169.24 (373,100)	2.3%
Payload	21.77 (48,000)	22.27 (49,100)	2%	36.42(4) (80,300)	67%
At Range = 9,200 km (4,968 NM) Fuel = 108.86 Mg (240,000 lbm)					
TOGW(3)	296.11 (652,800)	299.37 (660,000)	1%	314.52 (693,400)	6%
Fuel	108.86 (240,000)	108.59 (239,400)	−0.3%	100.20(5) (220,900)	−8%
At Range = 9,200 km (4,968 NM) Payload = 21.77 Mg (48,000 lbm)					
TOGW(3)	296.11 (652,800)	298.60 (658,300)	1%	291.21 (642,000)	−2%
Range - km (NM)	9,200 (4,968)	9,238 (4,988)	0.4%	10,645 (5,748)	16%
At Payload = 21.77 Mg (48,000 lbm) Fuel = 108.86 (240,000 lbm)					
TOGW(3)	296.11 (652,800)	298.85 (658,850)	1%	299.87 (661,100)	1%

Notes:
(1) Delta; change relative to baseline aircraft value
(2) Aircraft weight excluding payload and fuel
(3) Aircraft take-off gross weight
(4) Assumes a payload volume requirement equal to baseline
(5) Excludes effect of decrease in fuel volume requirements

TABLE 8

CRUISE FUEL FLOW SENSITIVITY

- Mach 6
- q = 23.9 kPa (500 psf) at L/D = 4.66
- q = 21.5 kPa (450 psf) at L/D = 5.83

Item	Change in Cruise Fuel Flow Rates*					
	Baseline Aircraft L/D = 4.66		Bare Aluminum Aircraft			
			L/D = 4.66		L/D = 5.83	
	(kg/s)	(lbm/sec)	(kg/s)	(lbm/sec)	(kg/s)	(lbm/sec)
1. Drag ~ Cold Wall Effects (1.7% Increase in Skin Friction)	—	—	0.062	0.137	—	—
2. Drag ~ Removal of External Shielding ($\Delta C_D = -0.0002$)	—	—	−0.152	−0.335	—	—
3. I_{SP} ~ Increase in Fuel Temperature	—	—	−0.379	−0.836	—	—
4. 25% Increase in Cruise (L/D)	—	—	—	—	−2.72	−6
Cruise Fuel Flow Rate	13.6	30	13.1	29	10.9	24
	Improvement*		3.4%		20%	

*Relative to baseline

"Page missing from available version"

page 34

CONCLUSIONS

Conclusions drawn from the present study are as follows:

1. With the aid of a large capacity heat pump it is technically feasible to cool to aluminum temperatures the airframe structure of an unshielded Mach 6 aircraft using the hydrogen fuel as the heat sink.
2. The use of a heat pump in lieu of shielding (external TPS) results in a 1.7% increase in aircraft empty weight. However, spinoff benefits in drag and specific impulse offset the mass gain and a small net improvement in aircraft performance is realized.
3. Substantial improvement in L/D (25%) can be readily accommodated with the heat pump concept. (Increasing L/D reduces the amount of fuel available for cooling).

"Page missing from available version"

page 36

RECOMMENDATIONS

It is recommended that additional studies be performed to:

1. Determine potential advantages of using a heat pump on other aircraft (including type, size, Mach number, and L/D).
2. Converge system for one aircraft to better define penalties/benefits to aircraft performance.
3. Determine optimum combination of shielding/heat pump requirements as a function of Mach number.
4. Assess impact of heat pump concept relative to descent/abort requirements.
5. Determine minimum mass heat pump system. Trade studies should include, (a) COP versus evaporator and condenser mass, (b) refrigerant versus evaporator and condenser mass, (c) hydrogen/glycol heat exchanger effectiveness versus heat pump mass, and (d) tube-shell versus plate-fin heat transfer devices.
6. Determine if unused (23%) hydrogen heat sink capacity can be effectively utilized.

APPENDIX

METHODOLOGY

Governing relations and methods used during the present study are discussed in the sections which follow.

POWER

As shown in various engineering textbooks, the change in enthalpy for a steady flow process with trivial changes in kinetic and potential energies is equal to the heat added minus the useful work (e.g. shaft work) done by the system. Hence, when the process is also adiabatic the amount of power (useful work per unit time) that can be extracted from the flow is equal to the fluid mass flow rate $\dot{m}_f$ times the change in enthalpy (h_2-h_1), as shown in equation 1.

$$\dot{W} = \dot{m}_f (h_2 - h_1) \qquad (1)$$

Turbines - Solving for the change in enthalpy for an adiabatic expansion of a perfect gas with constant specific heat (and substituting in equation 1) defines turbine power output (equation 2) as a function of mass flow rate, gas properties, fluid inlet temperature, and the pressure ratio across the turbine.

$$W_t = \dot{m}_f \left(\frac{R}{J}\right) \left(\frac{\gamma}{\gamma-1}\right) T_1 \left[1 - \frac{1}{PR^{(\gamma-1)/\gamma}}\right] \eta_t \qquad (2)$$

Turbine power output calculations performed during the present study were based on an adiabatic expansion efficiency η_t of 85%.

Compressors - An expression analogous to equation 2 defines compressor power requirements and is presented as equation 3.

$$W_c = -\left(\frac{\dot{m}_f}{\eta_c}\right) \left(\frac{R}{J}\right) \left(\frac{\gamma}{\gamma-1}\right) T_1 \left[PR^{(\gamma-1)/\gamma} - 1\right] \qquad (3)$$

Technically, as shown by equation 1 and 3, compressor power is negative because it is added to rather than extracted from the flow process. During this study, however, the sign convention was omitted and compressor (also pump) power requirements are

presented as positive values in the body of the report. Hydrogen and Freon compressor power requirements were computed based on an adiabatic compression efficiency η_c of 85% and 60%, respectively.

Pumps - For steady adiabatic flow of an incompressible fluid (liquid) the general expression for power (equation 1) takes the form of equation 4.

$$W_p = \frac{-\dot{m}_f (P_2 - P_1)}{\eta_p \rho} \qquad (4)$$

Pump power requirements were computed based on a pump efficiency of 85%.

The mass of the fuel pump was determined using the J-2 rocket's liquid hydrogen fuel pump as a data base (J-2 pump mass = 0.027 kg/kW; 0.045 lbm/HP). Methods used in computing the mass and volume of turbines and compressors is discussed in the section that follows.

TURBOMACHINERY CHARACTERISTICS

Turbines and compressors were sized (wheel diameter and rotational speed) based on the similarity concept discussed in references 7 through 9. Neglecting Mach and Reynolds number effects, similarity considerations show that the characteristics of turbomachines can be completely described by the parameters specific speed, N_s, and specific diameter, D_s, defined in equations 5 and 6, respectively.

$$N_s = \frac{NQ^{1/2}}{H^{3/4}} \qquad (5)$$

$$D_s = \frac{DH^{1/4}}{Q^{1/2}} \qquad (6)$$

where Q is the maximum volumetric flow and is therefore evaluated at the inlet for compressors and at the exit for turbines. That is,

$$Q_c = \dot{m}_f \, R \, T_1/P_1 \quad \text{(for compressors)} \tag{7}$$

$$Q_t = \frac{\dot{m}_f \, R \, T_1}{P_1} \, (PR)^{1/\gamma} \quad \text{(for turbines)} \tag{8}$$

The adiabatic head (the isentropic enthalpy change of the process, $\Delta h'$, times the mechanical equivalent of heat, J) can be expressed in terms of known conditions as presented in equations 9 and 10 for an adiabatic compression and expansion, respectively.

$$H_c = \frac{\gamma \, R \, T_1}{(\gamma - 1)} \left[PR^{(\gamma-1)/\gamma} - 1 \right] \tag{9}$$

$$H_t = \frac{\gamma \, R \, T_1}{(\gamma - 1)} \left[1 - 1/PR^{(\gamma-1)/\gamma} \right] \tag{10}$$

All turbomachines were sized as axial flow designs using the $N_s - D_s$ diagrams of references 7 and 9. Multi-stage designs were selected when the overall pressure ratio was greater than the maximum desired pressure ratio per stage as defined by equation 11.

$$PR_{max} = \left[\frac{1}{1 - \dfrac{V_T^{\,2} \, (\gamma-1)}{2g \, (V_T/C_o)^2 \, \gamma R \, T_1}} \right]^{\gamma/(\gamma-1)} \tag{11}$$

where,

V_T = wheel tip speed
C_o = spouting velocity = $(2g \, H_{st})^{1/2}$

To satisfy stress requirements, tip speeds were limited to 610 m/s (2000 ft/sec). The number of stages was determined from equation 12, where fractional parts were rounded to the next higher number.

$$n = \frac{\log PR}{\log PR_{max}} \tag{12}$$

The mass of turbomachine assemblies was determined using the "single wheel" correlation of reference 7, presented herein as equation 13.

$$\text{mass} = C_1 D^2 \tag{13}$$

where,

C_1 = 0.028 kg/cm^2 (0.4 lbm/in^2)
D = wheel diameter in cm (in.)

The mass of multi-stage assemblies was obtained by multiplying equation 13 by the number of stages.

Turbomachinery volume requirements were computed assuming a cylindrical assembly with dimensions as follows:

diameter = wheel diameter plus 2.54 cm (1.0 in.)
length = $L_1 + nL_2 + L_3$

where,

L_1 = allowance for bearings = 30.5 cm (12 in.)
L_2 = allowance per stage = 11.4 cm (4.5 in.)
n = number of stages
L_3 = allowance for exhaust system = 7.6 cm (3 in.)

HEAT PUMP CHARACTERISTICS

Following the procedure of reference 10, cycle performance of the heat pump was determined using a pressure - enthalpy plot for the selected refrigerant as illustrated in figure 8. As shown, the heat pump (vapor cycle refrigeration system) fluid experiences an increase in enthalpy equal to ($h_{2'} - h_{1'}$) as it absorbs heat at constant pressure in the evaporator. Between state points 1' and 2, the fluid absorbs heat via an isothermal phase change from a liquid to a vapor. Between state points 2 and 2', the vapor is superheated to ensure that no liquid enters the compressor. Area 2' - 3" - 3' is the increase in enthalpy and entropy resulting from the fact that the compression process (2' - 3") is nonisentropic and hence less than

100% efficient. The efficiency of the compression process is defined as follows:

$$\eta_c = \frac{h_3' - h_2'}{h_3'' - h_2'} \tag{14}$$

As suggested in reference 10, cycle performance for Freon R-11 refrigerant was determined based on a compression efficiency of 60%.

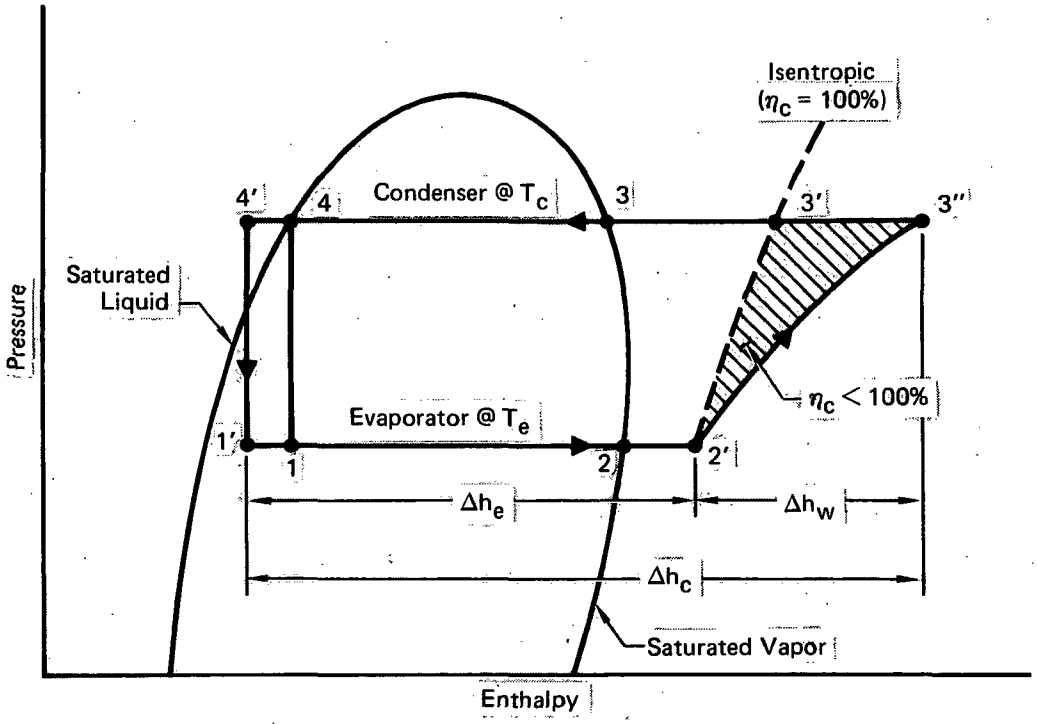

FIGURE 8
HEAT PUMP PERFORMANCE

Between 3'' and 4' the refrigerant is cooled (3'' - 3), condensed to a liquid (3-4), and subcooled (4-4') as heat is rejected in the condenser. Subcooling from 4-4' is necessary to ensure no flashing of liquid to vapor upstream of the expansion (throttle) valve. As the fluid expands at constant enthalpy through the throttle valve (4' - 1'), a portion of the liquid flashes to vapor and lowers the refrigerant temperature to the evaporation temperature T_e and completes the cycle.

For a given evaporator load $\dot{Q}_e$, the refrigerant mass flow rate $\dot{m}_R$ is determined knowing the change in enthalpy Δh_e across the evaporator, as illustrated in figure 8. That is

$$\dot{m}_R = \frac{\dot{Q}_e}{\Delta h_e} \tag{15}$$

The coefficient-of-performance (COP), a figure-of-merit used in assessing the relative efficiency of refrigeration cycles, is defined as the amount of refrigeration obtained per unit of work done on the system. The amount of refrigeration obtained is the evaporator load, $\dot{m}_R \Delta h_e$, and the amount of work done is $\dot{m}_R \Delta h_w$. Solving for Δh_w from the compression efficiency expression (equation 14), the coefficient-of-performance can be expressed as follows:

$$COP = \eta_c \left[\frac{h_2' - h_1'}{h_3' - h_2'}\right] \tag{16}$$

where the expression in brackets is the coefficient-of-performance of the cycle when the compression process is isentropic (see figure 8).

Refrigeration cycle state points for the Freon R-11 heat pump arrangement of figure 6 are presented in table 9.

Evaporator and condenser characteristics were determined by a computerized heat exchanger sizing program. Only tube - shell designs, with the refrigerant on the outside of finned tubes, were considered. Both aluminum and steel designs were assessed. In all cases, an aluminum design proved to be lighter in weight and was selected as the preferred concept.

The mass of Freon refrigerant in the system was determined assuming that the "free volume" in the evaporator and condenser was 25% liquid and 75% vapor.

TABLE 9
FREON R-11 REFRIGERATION CYCLE

- COP = 4
- η_c = 60%
- T_e = 318 K (573°R)
- T_c = 358 K (645°R)

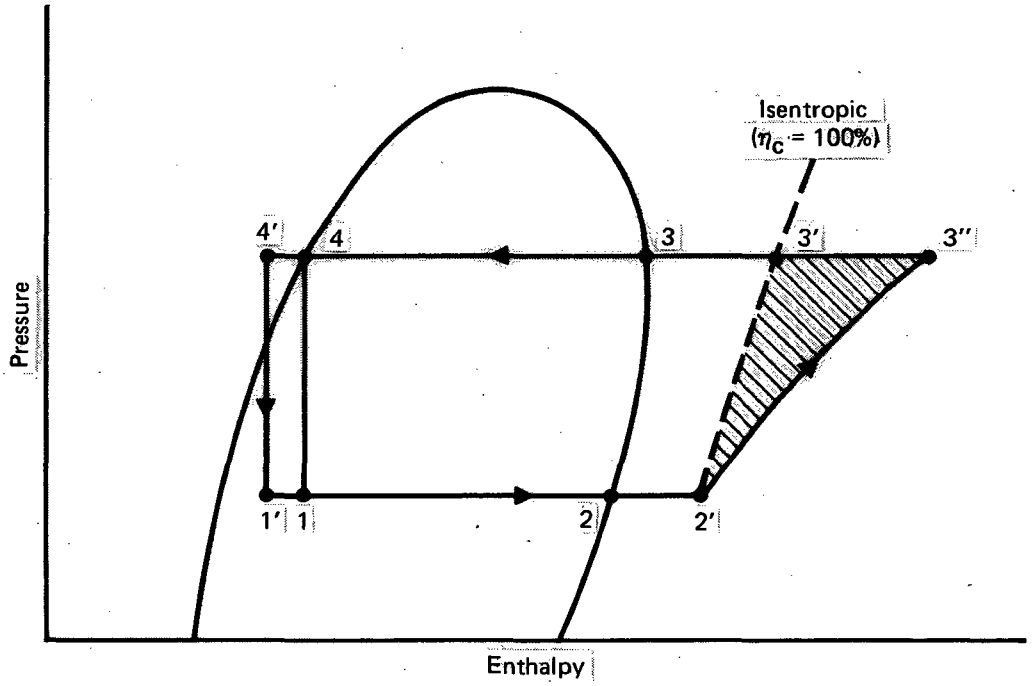

State Point	Temperature		Pressure		Enthalpy	
	K	°R	MPa	psi	J/g	Btu/lbm
1'	318	573	0.19	27.5	107	46
2	318	573	0.19	27.5	244	105
2'	322	580	0.19	27.5	249	107
3''	386	695	0.59	85.0	284	122
3'	368	662	0.59	85.0	270	116
3	358	645	0.59	85.0	263	113
4	358	645	0.59	85.0	109	47
4'	356	641	0.59	85.0	107	46

GEAR BOXES

The mass and power loss attributable to gear boxes were computed based on the results of previous in-house studies, as follows:

$$\text{mass} = 0.0125 \text{ kg/kW } (0.0206 \text{ lbm/HP}) \quad (17)$$

$$\text{power loss} = 1\% \text{ per gear mesh} \quad (18)$$

Gear box cooling requirements were assumed equal to the power loss defined by equation 18.

ACTIVE COOLING SYSTEM

The mass of the active cooling system was determined using the correlations of table 10. These correlations were derived during a previous MCAIR study of active cooling systems. Although derived specifically for a 60/40 mass solution of ethylene glycol and water, the correlations are believed to be equally applicable to other coolants.

AIRCRAFT PERFORMANCE

Performance characteristics of the bare aluminum aircraft were determined assuming a fixed aircraft size and adjusting baseline performance values for changes in mass, drag, and specific impulse; neglecting the effects of changes in payload and fuel volume requirements. Volume requirements of the heat pump system were also neglected as it occupies less than 1/2% of the baseline fuselage volume.

TABLE 10
EQUATIONS DEFINING THE MASS OF ACTIVE COOLING SYSTEM ELEMENTS

Mass Element	Equation ~ Mass/Area
(1) Pumps (Dual/Wet)	$W_1 = C_1\ (\dot{m}_c)\ (\Delta P_s)/\rho_c$
(2) Heat Exchanger (Wet)	$W_2 = C_2\ \dot{q}_{abs}$
(3) Coolant in Lines	$W_3 = C_3\ (\dot{m}_c)^{n1}\ (\mu_c)^{n2}\ (\rho_c)^{n3}\ \Delta P_s)^{n4}$
(4) Distribution Lines (Dry)	$W_4 = C_4\ (W_3)\ (P_s)/\rho_c$
(5) Reservoir (Wet)	$W_5 = C_5\ \Sigma$ Coolant Inventory • Coolant in Lines ~ W_3 • Coolant in H/X ~ 0.4 W_2 • Coolant in Panel ~ $\dfrac{C'_5\ (\rho_c)\ (D)^2}{P}$ Σ Coolant Inventory
(6) APS Propellant @ F = 0.34 g/kW·s (2 lbm/hp·hr)	$W_6 = C_6\ (\dot{m}_c)\ (\Delta P_s)\ (\theta)/\rho_c$

Variables			
Symbol	Definition	Units	
		SI	English
W_i	Mass Element	kg/m^2	lbm/ft^2
$\dot{m}_c$	Coolant Mass Flow	$kg/m^2 \cdot s$	$lbm/ft^2 sec$
P_s	System Pressure	kPa	$lbf/in.^2$
ΔP_s	Pressure Drop	kPa	$lbf/in.^2$
ρ_c	Coolant Density	kg/m^3	lbm/ft^3
$\dot{q}_{abs}$	Absorbed Heat Flux	kW/m^2	$Btu/ft^2 sec$
μ_c	Coolant Viscosity	Pa·s	lbm/ft sec
θ	Time	hour	hour
D	Dee Tube I.D.	cm	inch
P	Tube Pitch	cm	inch

Constants		
Symbol	Value in:	
	SI	English
C_1	0.44	0.19
C_2	0.0105	0.0244
C_3	2.49	3.9
C_4	0.116	0.05
C_5	0.06	0.06
C'_5	0.00467	0.0389
C_6	1.217	0.524
n_1	0.75	0.75
n_2	0.083	0.083
n_3	0.583	0.583
n_4	−0.417	−0.417

"Page missing from available version"

page 48

REFERENCES

1. Pirrello, C.J.; and Herring, R.L.: Study of a Fail-Safe Abort System for Actively Cooled Hypersonic Aircraft, NASA CR-2652, August 1976.
2. Program Review of, Thermal-Structural Design Study of an Airframe - Integrated Scramjet, Presented by Airesearch Company at NASA Dryden FRC, April 6, 1977. Contract NAS1-13984.
3. Becker, J.V.: New Approaches to Hypersonic Aircraft. Presented at the Seventh Congress of the International Council of the Aeronautical Sciences (ICAS), Rome, Italy, September 14-18, 1970.
4. Helenbrook, R.G.; and Anthony, F.M.: Design of a Convective Cooling System for a Mach 6 Hypersonic Transport Airframe, NASA CR-1918, December 1971.
5. Anthony, F.M.; Dukes, W.H.; and Helenbrook, R.G.: Internal Convective Cooling Systems for Hypersonic Aircraft, NASA CR-2480, February 1975.
6. Wieting, A.R.; and Guy, R.W.: Thermal-Structural Design/Analysis of an Airframe-Integrated Hydrogen Cooled Scramjet, Journal of Aircraft, Volume 13, Number 3, March 1976, p. 192.
7. Dieckman, R.R.; Watson, A.C.; and Glover, S.F.: Development of Integrated Environment Control System Designs for Aircraft, AFFDL-TR-72-9, Vol. I, May 1972.
8. Shepherd, D.C.: Principles of Turbomachinery, the Mac-Millan Company, 1956.
9. Balje', O.E.: A Study on Design Criteria and Matching of Turbomachines, Part A and Part B: Journal of Engineering for Power, January 1962, pp. 83 through 114.
10. SAE Aerospace Applied Thermodynamics Manual, Second Edition, October 1969, Society of Automotive Engineers, Inc.